N-Terminal Hydrophobic Residues of the G-Protein ADP-Ribosylation Factor-1 Insert into Membrane Phospholipids upon GDP to GTP Exchange†

Bruno Antonny,* Sophie Beraud-Dufour, Pierre Chardin, and Marc Chabre

CNRS, Institut de Pharmacologie Moleculaire et Cellulaire, 660 route des lucioles, 06560 Valbonne, France

Received September 6, 1996; Revised Manuscript Received November 18, 1996⊗

ABSTRACT: GDP/GTP exchange modulates the interaction of the small G-protein ADP-ribosylation factor-1 with membrane lipids: if ARF_{GDP} is mostly soluble, ARF_{GTP} binds tightly to lipid vesicles. Previous studies have shown that this GTP-dependent binding persists upon removal of the N-terminal myristate but is abolished following further deletion of the 17 N-terminal residues. This suggests a role for this amphipathic peptide in lipid membrane binding. In the ARF_{GDP} crystal structure, the 2−13 peptide is helical, with its hydrophobic residues buried in the protein core. When ARF switches to the GTP state, these residues may insert into membrane lipids. We have studied the binding of ARF to model unilamellar vesicles of defined composition. ARF_{GDP} binds weakly to vesicles through hydrophobic interaction of the myristate and electrostatic interaction of cationic residues with anionic lipids. Phosphatidylinositol 4,5-bis(phosphate) shows no specific effects other than strictly electrostatic. By using fluorescence energy transfer, the strength of the ARF_{GTP}−lipid interaction is assessed *via* the dissociation rate of $ARF_{GTP\gamma S}$ from labeled lipid vesicles. $ARF_{GTP\gamma S}$ dissociates slowly ($\tau_{off} \approx 75$ s) from neutral PC vesicles. Including 30% anionic phospholipids increases τ_{off} by only 3-fold. Reducing the N-terminal peptide hydrophobicity by point mutations had larger effects: F9A and L8A-F9A substitutions accelerate the dissociation of $ARF_{GTP\gamma S}$ from vesicles by factors of 7 and 100, respectively. This strongly suggests that, upon GDP/GTP exchange, the N-terminal helix is released from the protein core so its hydrophobic residues can interact with membrane phospholipids.

ARF[1] belongs to the superfamily of G-proteins that bind guanine nucleotides and adopt two different conformations, depending on whether GDP or GTP occupies the nucleotide site. In all G-proteins, the GTP-induced conformational change is the "on" signal that permits the G-protein to bind to and activitate specific protein effector targets (Bourne et al., 1991). Substitution of GDP by GTP induces large increases in G-protein affinities for their cognate effectors (Otto-Bruc et al., 1993; Herrmann et al., 1995). The effectors of ARF are not well-known. ARF is involved in the control of vesicular traffic in the golgi and regulates both phospholipase D and the binding of coatomer to budding vesicles (Moss & Vaughan, 1995). Despite the lack of information on ARF−effector interactions, there is no doubt that, as in ras, these interactions are regulated by a GTP-dependent "effector domain" formed by a loop−helix−loop motif, which switches the helix orientation upon GDP/GTP exchange. But in ARF, the GTP switch, besides controlling the interaction with effectors, has another effect: it induces the binding of ARF to membrane lipids. *In vitro*, in the presence of phospholipid vesicles, ARF_{GDP} is mainly found in solution, whereas ARF_{GTP} binds tightly to the vesicles (Walker et al., 1992; Franco et al., 1995).

Unlike ras, ARF is myristoylated at its N-terminus. The myristate is accessible for interacting with the lipids even when ARF is in the GDP-bound state: wild-type, myristoylated ARF_{GDP} binds moderately to azolectin vesicles, while unmyristoylated ARF_{GDP} shows no binding at all (Franco et al., 1995). Furthermore, the presence of lipid vesicles allows some spontaneous GDP to GTP exchange to occur in wild-type ARF but not in unacylated ARF. However, myristoylation alone cannot explain the GTP-dependent interaction of ARF with lipids: unacylated ARF_{GTP} binds to lipid vesicles and to PC−cholate micelles, whereas unacylated ARF_{GDP} does not (Franco et al., 1993). All these observations led to the hypothesis that ARF interacts with the membrane through two components: the myristate, which gives a basal affinity for lipid regardless of the protein conformation, and a protein region that becomes available for membrane binding only when ARF switches to the active, ARF_{GTP} conformation. The requirement of additional protein−membrane interactions for the tight binding of singly myristoylated proteins to lipid membranes has been recently demonstrated (McLaughlin & Aderem, 1995).

ARF displays a N-terminal extension that is not present in ras and is different from that found in any other small G-protein. The N-terminal peptide sequence $myrG_2$-NIFANLFKGLFGKK$_{16}$ suggests that it folds into an amphipathic helix, which could be the protein domain responsible for the GTP-dependent binding of ARF to lipids. $^{[\Delta 17]}$ARF, a mutant deleted of the first 17 residues (and of the attached myristoyl group), loses the GTP-dependent binding to lipids and remains soluble whatever the bound nucleotide (Kahn et al., 1992). Thus, the N-terminal peptide conformation must be affected by the GDP/GTP exchange

† This work was supported in part by grants from Ministère de l'Education Nationale: AC 1994 "Physico-chimie des membranes biologique" and ACC SV5 no. 9505025 "Interface chimie-physique-biologie". P.C. is supported by INSERM..

* Corresponding author. Phone: (33) 04 93 95 77 71. Email: antonny@unice.fr.

⊗ Abstract published in *Advance ACS Abstracts,* April 1, 1997.

[1] Abbreviations: ARF, ADP-ribosylation factor-1; DPH-PC, *β*-[3-(1,6-diphenyl-1,3,5-hexatrienyl)propanoyl]-*γ*-palmitoyl-L-α-phosphatidylcholine; PC, phosphatidylcholine; PG, phosphatidylglycerol; PS, phosphatidylserine; PIP_2, phosphatidylinositol 4,5-bisphosphate.

S0006-2960(96)02252-0 CCC: $14.00

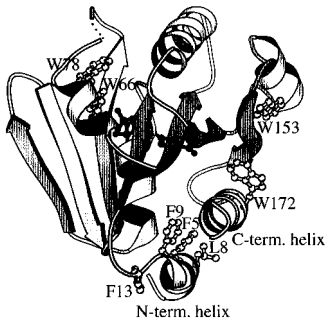

FIGURE 1: Ribbon diagram of ARF_{GDP}. This figure was generated by Molscript (Kraulis, 1991) using the coordinates of Amor et al. (1994). The N- and C-terminal helices are parallel and their axes are perpendicular to the plane of the figure. Leu^8 and the three phenylalanines (F^5, F^9, and F^{13}) of the N-terminal helix are shown. L^8 and F^9 have been mutated in this study. Note that these residues are not solvent exposed but buried in a pocket behind the C-terminal helix. The four trytophans of ARF are shown. Trp^{78} which corresponds to Trp^{207} in $G_t\alpha$ belongs to the "switch II" domain that is found in all G-proteins and must be responsible, at least partially, for the fluorescence change that is observed when GDP is replaced by GTP.

to control the binding of ARF_{GTP} to lipids. How this ARF specific GDP/GTP switch works is not known. Does the N-terminal peptide bind directly to lipids as a consequence of the GTP-induced conformational change? Does it simply control the exposure of the covalently attached myristate? Some confusion has arisen from the suggestion that this N-terminal domain might also be involved in the interactions of ARF with its effector proteins, based on the observation that the deletion affects also the activity of ARF on these effectors proteins. But this is probably only a side effect of the lack of binding of $^{[\Delta 17]}ARF_{GTP}$ to membranes where ARF_{GTP} normally interacts with its effectors.

The crystallographic stucture of GDP-bound, unmyristoylated ARF has been recently solved (Amor et al., 1994; Greasey et al., 1995). As expected, the N-terminal peptide folds as an amphipathic helix that binds the protein core *via* hydrophobic contacts (Figure 1). The hydrophobic residues I^4, F^5, L^8, F^9, and L^{12} point inward, into a hydrophobic pocket that does not seem to leave room for the myristate to fold inside. Thus, when ARF is in the GDP state, these N-terminal hydrophobic residues cannot interact with membrane lipids. Our working hypothesis is that, upon the GDP/GTP exchange, the N-terminal helix is released from the protein core hydrophobic pocket and switches to expose its hydrophobic residues to the membrane. The insertion of the three repeats of hydrophobic residues (IF or LF) into the lipid layer, in addition to the myristoyl group, would then stabilize the association of ARF_{GTP} with lipid membranes.

So far, the interaction of ARF with membranes has been studied by using DMPC−cholate micelles or azolectin (soybean lipid) large unilamellar vesicles as model membranes. Therefore, little information concerning the physical basis of ARF−membrane interaction is available. Some effects of PIP_2 on ARF have been reported, but they were observed upon addition of high concentrations of pure PIP_2 to a PC/cholate mixture (Terui et al., 1994). In this study, we have used "extruded" unilamellar vesicles of defined size and homogeneous composition in order to control and study the contributions of hydrophobic, electrostatic, and possible PIP_2 specific interactions in the binding of ARF_{GDP} and $ARF_{GTP\gamma S}$ to membranes. This type of vesicle has already been used as model membranes in many recent quantitative studies of protein−membrane or peptide−membrane interactions (Peitzch & McLaughlin, 1993; Silvius & L'Heureux, 1994; Sigal et al., 1994; Vergeres et al., 1995; Lu & Nelsestuen, 1996; Ktistakis et al., 1996). This will provide comparisons between different proteins in their interaction with membrane. To test our hypothesis that N-terminal hydrophobic residues contribute specifically to the GTP-dependent binding of ARF to membranes, we modulated the hydrophobicity of the N-terminal amphipatic helix of ARF by point mutations, replacing large hydrophobic residues with alanine. We tested the effects of such changes on the binding of ARF_{GTP} to the unilamellar lipid vesicles. The exchange of GDP for GTP (or GTPγS), which is also dependent on the interaction of ARF with the lipids, was followed by monitoring the associated change of tryptophan fluorescence. To quantify the interaction of $ARF_{GTP\gamma S}$ with lipids vesicles, we developed a fluorescence energy transfer technique which allowed us to monitor, in real time, the translocation of $ARF_{GTP\gamma S}$ from fluorescent-labeled vesicles to unlabeled ones. Since the rate of $ARF_{GTP\gamma S}$ desorption from lipid vesicles reflects the "strength" of the interaction, the effects of lipid composition, of lipid charge density, and of ARF point mutations or deletions on the interaction of $ARF_{GTP\gamma S}$ with a lipid membrane can be quantified. Our results show that this interaction is mainly hydrophobic and suggest that it is due to the insertion in the membrane lipid hydrophobic layer of the hydrophobic residues of the N-terminal helix of ARF that become exposed in the "active" GTP-bound state.

MATERIAL AND METHODS

Materials. Egg phosphatidylcholine (PC), egg phosphatidylglycerol (PG), brain phosphatidylserine (PS), and phosphatidylinositol 4,5-bis(phosphate) were purchased from Sigma. β-[3-(1,6-Diphenyl-1,3,5-hexatrienyl)propanoyl]-γ-palmitoyl-L-α-phosphatidylcholine (DPH-PC) and other fluorescent phospholipid analogs were from Molecular Probes.

Proteins. Myristoylated and unmyristoylated ARF were prepared as described (Franco et al., 1993, 1995). The truncated mutant of ARF, $^{[\Delta 17]}$ARF, and the N-terminal mutant [Trp^9]ARF ($^{[F9W]}$ARF), in which Phe^9 is replaced by a tryptophan, were prepared by polymerase chain reaction amplification of the bovine rARF1 cDNA. For $^{[\Delta 17]}$ARF, the following primers were used:

5′-AAACATATGCGCATTCTCATGGTGGGCCTA-3′
(oligonucleotide 1)

5′-ATGAGGATCCTCATTTCTGGTTCCGGAGCT-3′
(oligonucleotide 2)

Oligonucleotide 1 introduces a *Nde*I site at the initiating codon, and oligonucleotide 2 includes a *Bam*H1 site after the stop codon. The *Nde*I-*Bam*HI fragment was inserted in the pET11a expression vector (Novagen Inc.).

For $^{[F9W]}$ARF, oligonucleotide 2 was identical, and oligonucleotide 1 was

5′-TATACCATGGGGAATATCTTTGCAAA-
CCTCTGGAAAGGCCTTTTT-3′

This primer includes an *Nco*I site and introduces the F/W mutation and an *Stu*I site which does not change amino acid sequence.

Two mutants, [Ala^9]ARF ($^{[F9A]}$ARF) and [Ala^8,Ala^9]ARF ($^{[L8A-F9A]}$ARF), were prepared from the $^{[F9W]}$ARF mutant by replacing the *Nco*I-*Stu*I fragment by sense and antisense oligonucleotides that include the desired mutation. The *Nco*I-*Bam*HI fragment was inserted in the pET11d expression vector (Novagen Inc.).

$^{[\Delta 17]}$ARF was expressed in *Escherichia coli* and purified on an ACA 44 (Ultrogel) gel filtration column. Wild-type ARF1 and the three mutants, $^{[F9W]}$ARF, $^{[F9A]}$ARF, and $^{[L8A-F9A]}$ARF, were expressed in *E. coli* with yeast *N*-myristoyl transferase and purified in the myristoylated form as described (Franco et al., 1995). Briefly, myristoylated ARF is purified through three steps: (i) precipitation at 35% saturation ammonium sulfate of the supernatant obtained after bacteria lysis; (ii) DEAE-Sepharose chromatography; (iii) MonoS chromatography (Pharmacia). Myristoylated ARF is detected, by SDS−PAGE, as a band of greater mobility than that of unmyristoylated ARF. Myristoylated wild-type and mutated proteins were >95% pure. For each mutant, the N-terminal sequence of the unmyristoylated form was determined by Edman degradation. Protein concentrations were determined by a coomassie assay.

Vesicle Preparation. Unilamellar vesicles were prepared by the extrusion method of Hope et al. (1985). These vesicles are unilamellar, so that exactly half of their phospholipids are accessible for protein binding, and thanks to their relatively uniformly small size, light scattering is low; thus, they do not interfere, even at high concentration (10^{-4}−10^{-3} M) with fluorescence assays.

Solutions of PC, PG, and PS in chloroform and PIP_2 in chloroform:methanol:H_2O:HCl (1N) (20:9:1:0.1) were mixed in the required proportion. When PIP_2 was used, the chloroform:methanol 2:1 ratio was maintained in the mixture to allow homogenous mixing of the PIP_2 and the other lipid solutions. A film was formed in a rotavapor and resuspended in 50 mM HEPES pH 7.5 and 100 mM KCl. The suspension was vortexed for 20 min and then freeze−thawed five times. Unilamellar vesicles were produced by extrusion through a 0.1 μm pore size polycarbonate filter (isopore, Millipore) using an extrusion apparatus similar to the one described by MacDonald et al. (1991). For sucrose-loaded vesicles, the same procedure was used except that the buffer was 220 mM sucrose, 20 mM Tris, pH 7.5, and that 0.4 μm pore size polycarbonate filters were used. After extrusion, the sucrose-loaded vesicles were diluted five times in 20 mM Tris, pH 7.5, and 120 mM NaCl, centrifuged for 10 min at 400000*g*, and resuspended in the same buffer before use. The phospholipid concentration was determined using a Fiske−Subbarow phosphorus assay.

Sedimentation Experiments. ARF_{GDP} (2 μM) either myristoylated or not was incubated for 15 min at 25 °C with sucrose-loaded vesicles in 20 mM Tris, 120 mM NaCl, 1 mM $MgCl_2$, 1 mM DTT, and a submicellar concentration of Thesit [dodecyl poly(ethyleneglycol ether)$_n$ 10 μM] to prevent ARF retention on the tube walls. The tubes were centrifuged for 10 min at 400000*g* and 25 °C. The percentage of ARF_{GDP} in the supernatant was determined by densitometry of SDS−PAGE.

Fluorescence Measurements. Tryptophan fluorescence was used to follow ARF conformational change upon GDP to GTP exchange. A large increase in the intrinsic fluorescence of ARF occurs when GDP is exchanged for GTP or GTPγS (Kahn & Gilman, 1986). This signal is reminiscent of the one observed with heterotrimeric G-proteins (Higashijima al., 1987; Faurobert et al., 1993). Fluorescence energy transfer from the tryptophans of ARF to the fluorescent phospholipid analog DPH-PC, was used to follow the binding of ARF to vesicles.

All fluorescence measurements were performed with a Shimadzu RF-5000 fluorimeter in a 6 mm diameter cylindrical quartz cell. The sample (600 μL) was thermostated at 37 °C and continuously stirred with a magnetic bar. Injections were done with Hamilton syringes. With vigorous stirring, the mixing time was ≈0.5 s. The time constant of the fluorimeter was set according to the kinetics studied, down to 125 ms for fast kinetic measurements. The sample buffer was 50 mM HEPES, pH 7.5, 120 mM KCl, 1 mM $MgCl_2$, and 2 mM DTT. When indicated, magnesium was chelated by 2 mM EDTA ($[Mg^{2+}]_{free} \approx 1$ μM). As for other small GTP-binding proteins such as ras or rab, the chelation of magnesium accelerates the dissociation of GDP from ARF and thus facilitates its replacement by GTPγS (Antonny et al., 1991; Franco et al., 1993, 1995).

For tryptophan fluorescence, the excitation and emission wavelengths were 297.5 and 340 nm, respectively. Artifactual contributions from light scattering by unilamellar vesicles were subtracted. For fluorescence transfer measurements, unilamellar vesicles containing 5% of DPH-PC were used. Tryptophans were excited at 280 nm, and the emission of DPH-PC was monitored at 460 nm. The fluorescence energy transfer is expressed as a percentage change from the fluorescence of the vesicles before the binding of ARF and due to the direct excitation of the DPH-PC probe by 280 nm light.

For all fluorescence measurements, large emission bandwidths (10−30 nm) and small excitation bandwidths (1.5−5 nm) were used to maximize the signal:noise ratio.

Nucleotide Binding Assay. The binding of [^{35}S]GTPγS (1200 cpm/pmol) to ARF was measured as described by Franco et al. (1995) under experimental conditions (buffer, vesicles) identical to those used for fluorescence measurements.

Data Analysis. All kinetics data were fitted to single exponentials. In some fluorescence transfer experiments, a negative slope was added to the fit to account for the slow decay of the fluorescence (probably due to photobleaching). Small variations (<±10%) in the value of the time constant (τ_{off}) for $ARF_{GTP\gamma S}$ transfer from labeled to unlabeled vesicles were observed when determined from duplicate or triplicate experiments using the same batch of vesicles. Larger (<±25%) variations were observed when different preparations of vesicles of the same composition were used. Therefore, we consider that these τ_{off} values are known with a precision of ±25%. Since each mutant was compared to the wild-type protein by using the same batch of vesicles, the ratio of τ_{off} values for wild-type and each mutant is known with an accuracy of about ±10%.

ARF activation as a function of phospholipid concentration can be seen as a partitioning process between the soluble ARF_{GDP} form and the membrane-bound $ARF_{GTP\gamma S}$ form. This can be analyzed with the following equilibria:

$$ARF_{GDP} + PL + GTP\gamma S \overset{K_1}{\leftrightarrow} ARF_{GTP\gamma S}-PL + GDP \quad \text{(reaction 1)}$$

$$ARF_{GDP} + PL_n + GTP\gamma S \overset{K_2}{\leftrightarrow} ARF_{GTP\gamma S}{-}PL_n + GDP \quad \text{(reaction 2)}$$

The corresponding equations are

$$[ARF_{GTP\gamma S}{-}PL] = A_T[PL]_{free}/(K_1 + [PL]_{free}) \approx A_T[PL]_{eff}/(K_1 + [PL]_{eff}) \quad (1)$$

$$[ARF_{GTP\gamma S}{-}PL_n] = 0.5\{A_T + [PL]_{eff}/n + K_2 - [(A_T + [PL]_{eff}/n + K_2)^2 - 4A_T[PL]_{eff}/n]^{1/2}\} \quad (2)$$

A_T is the total concentration of ARF, $[PL]_{eff}$ is the concentration of surface-exposed phospholipids (half of the total concentration), and $[PL]_{free}$ is the concentration of surface-exposed phospholipids that are free, i.e., not masked by an $ARF_{GTP\gamma S}$ molecule. In reaction 1, ARF is assumed to interact with one phospholipid (PL) and with an equilibrium constant, K_1. This constant corresponds to a molar partition coefficient between the aqueous phase and the membrane phase. Its value can be compared to that obtained for other membrane-associated proteins or peptides.[2] Equation 1 can be used when the phospholipid concentration is several orders of magnitude higher than that of the protein ($[PL]_{free} \approx [PL]_{eff}$). However, when the molar ratio of phospholipids versus ARF that allows ARF activation and binding is relatively low (10−100), the membrane surface occupied by each ARF molecule lowers the concentration of accessible phospholipids ($[PL]_{free} < [PL]_{eff}$). Therefore, a more realistic scheme for the interaction of ARF with the membrane must be considered, where ARF interacts in a 1:1 stochiometry with a membrane patch formed by n phospholipids (PL_n) and with an equilibrium constant K_2 (reaction 2). Fitting the dose−response curve with the corresponding quadratic equation (eq 2) gives the two parameters n and K_2. The molar partition coefficient K_1 is determined by $K_1 = nK_2$. Note that reactions 1 and 2 decribe a partitioning process between two different conformations. Therefore, K_1 and K_2 do not give the real "affinity" of the GTPγS bound form of ARF for lipids but rather an upper limit for the the molar partition coefficient of this form.

RESULTS

Roles of the Myristate and of Electrostatic Interactions in the Binding of ARF_{GDP} to Phospholipids. The binding of ARF_{GDP} to phospholipid vesicles was studied by its cosedimentation with sucrose-loaded vesicles (Figure 2). ARF_{GDP} binding to vesicles is significant only at high lipid concentrations (millimolar) and depends on both myristoylation and vesicle surface charge density. No significant binding is detectable when ARF is not myristoylated or when no anionic lipids (PG) are included in the vesicles. Thus, the interaction of the GDP-bound form of ARF with membranes is weak and involves both charge−charge interactions and the hydrophobic interaction of the myristate with the bilayer. Similar results were obtained in the presence of a high concentration (500 μM) of GDP to prevent the formation of the empty state. This suggests that ARF remains predominantly in the GDP-bound state when interacting with vesicles.

[2] For a discussion on the coefficients that are used to characterize the partitioning of peptides and proteins onto membranes, see Peitzsch and McLaughlin (1993) and Silvius and l'Heureux (1994).

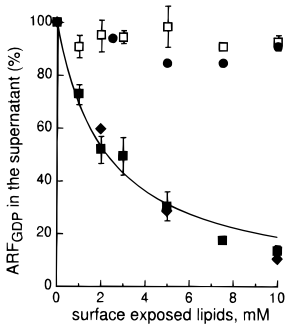

FIGURE 2: Binding of myristoylated and unmyristoylated ARF_{GDP} to neutral or charged lipid vesicles. ARF_{GDP}, either myristoylated (□, ■, ◆) or not (●), was incubated with sucrose-loaded vesicles countaining 100% PC (□) or 70% PC and 30% PG (■, ●, ◆) and in the presence (◆) or in the absence (□, ■, ●) of 0.5 mM GDP. After centrifugation, the percentage of ARF in the supernatant was determined and plotted as a function of the concentration of surface-exposed lipids (50% of total). Error bars correspond to two independent experiments.

It has been proposed that ARF has a specific binding site for PIP_2 and that this phospholipid acts as a guanine nucleotide exchange factor for ARF by stabilizing its empty conformation (Terui et al., 1994). We looked for an effect of PIP_2 on the binding of ARF_{GDP} to vesicles. The inclusion of 5% PIP_2 in either pure PC or PC:PG 70:30 vesicles did not significantly increase the binding of ARF_{GDP} (data not shown).

Stimulation of GDP/GTP Exchange on ARF by Lipid Vesicles. ARF cannot switch to the active GTP-bound state in the absence of membrane. This reflects the fact that the GTP-bound state is stable only when associated to membrane lipids (Walker et al., 1992; Franco et al., 1995; Randazzo et al., 1995). Thus, as a preliminary to the study of the ARF−lipid interaction, we have studied the dependency of ARF activation, upon GDP/GTPγS exchange, on the composition and on the concentration of the lipid vesicles. The final extent of GDP/GTPγS exchange must depend on the "tightness" of the interaction between $ARF_{GTP\gamma S}$ and lipids. In addition, the initial rate of GDP/GTP exchange also depends on the interaction of the GDP-bound form of ARF with membrane lipids, since this weak interaction favors GDP release (Franco et al., 1995). ARF conformational change upon GDP to GTPγS exchange was followed in real time by monitoring the correlated increase in ARF tryptophan fluorescence (Kahn & Gilman, 1985). This signal is probably due to Trp^{78}, which corresponds to the conserved tryptophan of the switch II domain of G-protein α subunits whose fluorescence is increased upon GTP binding (Faurobert et al., 1993).[3]

In Figure 3A, ARF_{GDP} is injected in a fluorescence cuvette containing various concentrations of unilamellar PC vesicles. A 20-fold excess of GTPγS is then added, followed by the addition of 2 mM EDTA. Lowering the concentration of free magnesium from the millimolar to the micromolar range facilitates GDP dissociation and hence guanine nucleotide exchange. In the absence of vesicles, the addition of EDTA

[3] In addition to Trp 78, other tryptophans may also contribute to the fluorescence change. In the structure of ARF_{GDP}, Trp 78 is not solvent-exposed as in the case of $transducin_{GDP}$ but is very close to another Trp at position 66 (Amor et al., 1994). The relative movement of the two Trp 66 and 78 upon GDP to GTP exchange could modify the reciprocal quenching between these two residues.

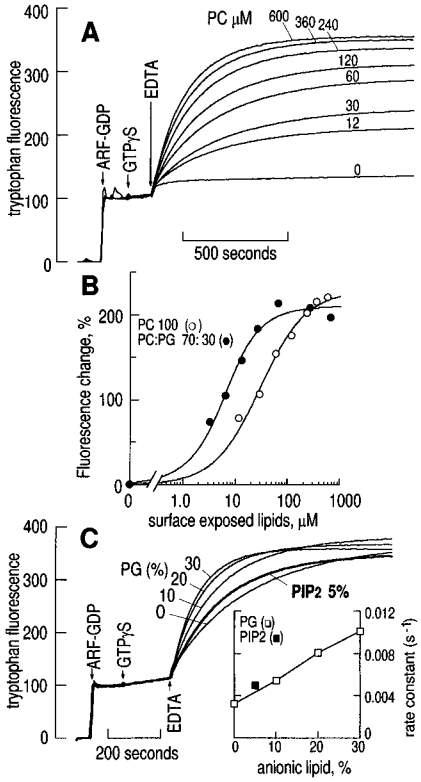

FIGURE 3: Stimulation of GDP/GTP exchange in myristoylated ARF by lipid vesicles. (A) GDP to GTPγS exchange was monitored by the correlated variation in tryptophan fluorescence. ARF_{GDP} (0.25 μM) was injected in a fluorescence cuvette containing various amounts of PC vesicles in buffer with 1 mM $MgCl_2$. At the indicated times, GTPγS (20 μM) and EDTA (2 mM) were added to promote GDP release and its substitution by GTPγS. For each measurement, the concentration of accessible phosphatidylcholine (50% of total) is given. Light scattering from vesicles was subtracted. (B) The amplitude of the fluorescence change upon GDP to GTPγS exchange was plotted as a function of PC concentration (open circles). The filled circles show the dose−response curve obtained with PC:PG (70:30%) vesicles. The data points are fitted according to eqs 1 or 2 (see Materials and Methods), and the following parameters were found: PC vesicles (○), K_1 (molar partion coefficient) = 30 μM; PC:PG vesicles (●), $n = 22$, $K_2 = 0.16$ μM and $K_1 = 3.6$ μM. (C) Effect of lipid surface charge density on the rate of myrARF activation. ARF activation upon GDP to GTPγS exchange was measured as in panel A in the presence of PC vesicles with increasing percentages of PG or PIP_2. The concentration of phospholipid was held constant (400 μM accessible phospholipids). Inset: rate constant of ARF activation as a function of percent PG or PIP_2.

has no effect except for a small (≈10%) instantaneous fluorescence increase, which probably reflects the dissociation of magnesium from the nucleotide site. In the presence of PC vesicles, the addition of EDTA promotes a fluorescence increase with a typical exponential shape whose kinetics correlates with that of GTPγS binding as measured under the same conditions with radiolabeled GTPγS (see below). Thus, ARF can switch to the GTPγS-bound state in the presence of neutral phosphatidylcholine vesicles. The amplitude of the fluorescence change is proportional to the amount of ARF that has switched to the GTPγS bound state and is plotted as a function of the concentration of exposed lipids (Figure 3B). Half-maximal activation is observed with 30 μM PC. This concentration is low when compared with that required for the binding of two well-studied myristoylated proteins, MARKCS and Src (Kim et al., 1994; Vergeres et al., 1994; Sigal et al., 1994). These proteins interact with neutral PC vesicles through the insertion of the myristate and exhibit apparent affinities for PC in the millimolar range. The fact that a much lower concentration of PC suffices for ARF activation by GTP suggests that the tight binding of ARF_{GTP} to neutral vesicles involves hydrophobic amino acids in addition to the myristate.

The effect of acidic phospholipids was then investigated (Figure 3B). With 30% phosphatidylglycerol (PG) and 70% PC, the dose−reponse curve is shifted to ≈5 times lower concentrations of lipid, compared with that obtained with pure PC vesicles. This suggests the involvement of electrostatic interactions between $ARF_{GTP\gamma S}$ basic residues and acidic phospholipids. These interactions are not specific of the PG polar head since similar results are obtained when PS is added instead of PG (data not shown). Fitting the dose−response curve with an equation describing the interaction of $ARF_{GTP\gamma S}$ with membrane (see Materials and Methods) shows that each $ARF_{GTP\gamma S}$ occupies a membrane area corresponding to $n \approx 20-25$ phospholipids, that is ≈15−20 nm^2. Given the size of ARF ($4.8 \times 3.8 \times 3.7$ nm^3; Greasey et al., 1995), this corresponds to a very close packing of the proteins on the membrane surface.

Since ARF activation is rate-limited by GDP release, any effect of phospholipids on the activation rate must be due to the interaction of ARF_{GDP} with lipids. This rate depends on lipid concentration as well as on composition. At high phospholipid concentrations (400 μM accessible phospholipids), ARF activation is complete even with pure PC vesicles (Figure 3B); thus, only the rate of ARF activation can be affected by vesicles composition. Incorporating 30% of the anionic lipid PG increases guanine nucleotide exchange rate 3-fold (Figure 3C). This suggests that some charge−charge interactions between ARF_{GDP} and the membrane facilitate GDP release. On this time scale, nearly no nucleotide exchange is detected with nonmyristoylated ARF, in agreement with our earlier observation (Franco et al., 1995) that the myristate is crucial for the interaction of ARF_{GDP} with the membrane and favors ARF activation. Thus, both myristate and charges are involved in ARF_{GDP} membrane interaction, confirming the results of sedimentation experiments.

We also looked for an effect of PIP_2 on the activation of ARF. Including 5% PIP_2 in PC vesicles slightly accelerates ARF activation (Figure 3C), but this effect is weak and similar to that observed with 5−10% of any other anionic lipids (PG, PS). Thus, PIP_2 does not act as a specific opener of ARF guanine nucleotide site. We have shown elsewhere (Chardin et al., 1996) that PIP_2 increases indirectly the rate of ARF activation by promoting the binding to membranes of ARNO, the exchange factor of ARF. Other lipids, phosphatidylethanolamine, phosphatidic acid, diphosphatidylglycerol, ceramides, diacylglycerol, and cholesterol, were also incorporated at 10−30% in PC vesicles and tested for their effects on ARF activation. Some effects on the rate and/or on the extent of ARF activation were observed. But these effects are always weak (less than a factor of 2).

Fluorescence Transfer Measurements of ARF Binding to and Dissociation from Lipid Vesicles. To quantify the interaction of $ARF_{GTP\gamma S}$ with membranes, we developed a fluorescence energy transfer assay to follow in real time the binding of ARF to vesicles. We labeled the lipid vesicles with a few percent fluorescent phospholipid analogs. We tested several phospholipid probes, either extrinsic (dansyl-

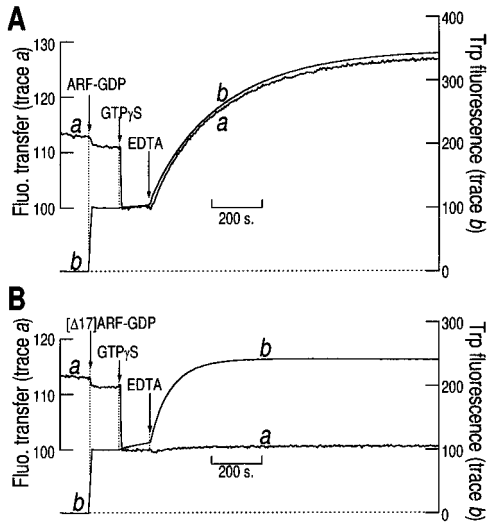

FIGURE 4: Fluorescence energy transfer measurement of the binding of ARF to phospholipid vesicles. (A) Trace *a* shows the time course of ARF binding to vesicles as monitored by fluorescence energy transfer from ARF tryptophans to the fluorescent phospholipid probe, DPH-PC (excitation = 280 nm, emission = 460 nm). Trace *b* shows the time course of ARF conformational change measured, under the same experimental conditions, by intrinsic tryptophan fluorescence (excitation = 297.5 nm, emmission 340 nm). Myristoylated ARF_{GDP} (0.5 μM) was injected in a fluorescence cuvette containing PC:PG vesicles (30% PG) labeled (trace *a*) or not labeled (trace *b*) with 5% DPH-PC in buffer with 1 mM $MgCl_2$. The total phospholipid concentration was 125 μM. An excess of GTPγS (20 μM) was then added and, as in Figure 3, ARF activation was triggered by the addition of 2 mM EDTA. To facilitate kinetics comparison, trace *b* was scaled by an appropriate factor and superimposed on trace *a*. (B) The same experiments as in panel A were carried out with the truncated mutant of ARF, $^{[\Delta 17]}$ARF. The same scale factor as in panel A was used to superimpose the fluorescence transfer (*a*) and trytophan fluorescence (*b*) recordings. $^{[\Delta 17]}$ARF is activated by GDP/GTPγS exchange (trace *b*) but does not bind to the fluorescent labeled vesicles (trace *a*).

PE) or intrinsic [(diphenylhexatriene)-PC and dipyrene-PC derivatives]. These probes exhibit excitation spectra that overlap the tryptophan emission spectrum and hence could be excited by ARF tryptophans, when ARF becomes membrane bound. With all these probes, a fluorescence transfer was detected. The largest signal was observed with DPH-PC, which was used in all the experiments shown.

Trace *a* in Figure 4A shows a typical fluorescence transfer measurement. The fluorescence of PC:PG:DPH-PC vesicles (65:30:5, total phospholipid concentration = 125 μM) is continuously monitored with tryptophan excitation at 280 nm and DPH-PC emission at 460 nm. As expected, the addition of ARF_{GDP} has no effect: at this lipid concentration, ARF_{GDP} remains essentially in solution (see Figure 2) and therefore cannot transfer energy to the lipid probe. Activation of ARF is then triggered by the sequential additions of GTPγS and EDTA. The addition of GTPγS induces an instantaneous fluorescence decrease due to its UV absorbance. After the addition of EDTA, an exponential increase is observed. Several lines of evidence show that this signal is due to fluorescence energy transfer from ARF tryptophans to the phospholipid probe. First, no fluorescence change is detected when the phospholipid probe is directly excited at 350 nm. Second, the signal amplitude is proportional to the concentration of ARF used. Third, the amplitude is reduced by ca. 50% when unlabeled vesicles are added in the assay in the same amount than labeled vesicles, showing that labeled and unlabeled vesicles compete equally for the binding of ARF-GTPγS.

The rate at which ARF binds to the vesicles corresponds to the rate at which it switches to the active GTPγS-bound state. Trace *b* in Figure 4A shows the time course of ARF activation. The experimental conditions are identical to those used for the previous fluorescence transfer measurement, except that the vesicles are not labeled and ARF activation is monitored by direct tryptophan fluorescence. The two fluorescence recordings (*a* and *b*) exhibit exponential changes with indistinguishable characteristic times. Thus, the conformational change of ARF upon GDP to GTPγS exchange, as monitored by tryptophan fluorescence, and the binding of ARF to vesicles, as monitored by fluorescence transfer, are strictly correlated in time.

Further control experiments were carried out with $^{[\Delta 17]}$ARF (Figure 4B). This mutant lacks the myristate and the 17 N-terminal residues and has been shown to remain soluble whatever the bound nucleotide and to display guanine nucleotide exchange activities that are independent of the presence of phospholipids (Kahn et al., 1992; Randazzo et al., 1995). Upon additions of GTPγS and EDTA, a large enhancement in $^{[\Delta 17]}$ARF tryptophan fluorescence is observed (trace *b*), confirming that the mutant switches to the active GTPγS state. But no corresponding fluorescence transfer is detected from the $^{[\Delta 17]}$ARF tryptophans to the lipid probes (trace *a*), as $^{[\Delta 17]}ARF_{GTP\gamma S}$ does not bind to the vesicles. This confirms the importance of the N-terminal residues for the GTP-dependent binding of ARF to membranes.

The rate of $ARF_{GTP\gamma S}$ dissociation from vesicles was determined by monitoring the translocation of $ARF_{GTP\gamma S}$ from DPH-PC-labeled vesicles to an excess of unlabeled vesicles. A typical experiment is shown in Figure 5A. ARF is activated by GTPγS at low [Mg] and its binding to neutral, PC:DPH-PC (95:5) vesicles is monitored by fluorescence transfer to the lipid probe (trace *a*, Figure 5A). When the exchange is complete, magnesium is added back to stabilize the bound GTPγS. At the time indicated, a 5-fold excess of unlabeled vesicles is added: this addition induces a fluorescence decay with an amplitude equal to that of the "binding" signal and with a time constant of 75 $\pm$ 15 s. A second injection of unlabeled vesicles has no effect except for a light scattering injection artifact. We have checked that the decay in fluorescence energy transfer after the first addition of unlabeled vesicles monitors the translocation of the GTPγS bound form of ARF from labeled to unlabeled vesicles and not the replacement of GTPγS by GDP in ARF: recordings of ARF tryptophan fluorescence and of [^{35}S]GTPγS binding under experimental conditions similar to those used for fluorescence energy transfer show no change in the fluorescence of the protein and in the binding of GTPγS when the 5-fold excess of vesicles is added.

Similar experiments were carried out with vesicles containing anionic phospholipids, and the off rates are shown in Figure 5B. In the presence of 30% PG or PS, $ARF_{GTP\gamma S}$ dissociation from the vesicles is slowed down by a factor of $\approx$3 (τ = 225 $\pm$ 25 s). PIP_2 (10%) has an effect comparable to that of PS or PG.

Mutations of the N-Terminal Helix: Effects on the GDP/GTP Exchange and on the Dissociation of $ARF_{GTP\gamma S}$ from Lipid Vesicles. The observation that $ARF_{GTP\gamma S}$ dissociates slowly even from neutral vesicles prompted us to examine whether hydrophobic residues, besides the myristate, could

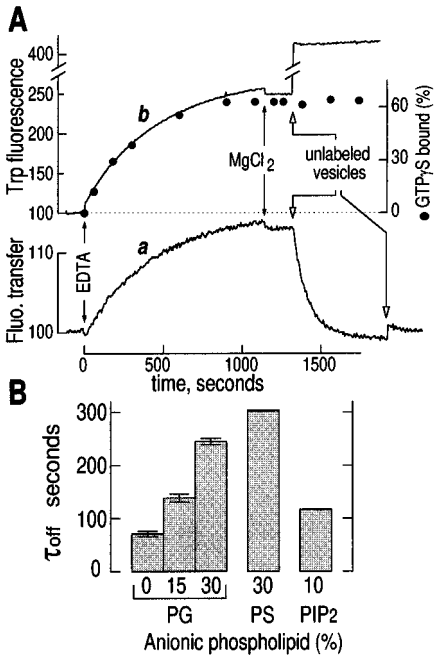

FIGURE 5: $ARF_{GTP\gamma S}$ dissociation from vesicles. (A) Trace *a* shows a typical measurement of the dissociation of $ARF_{GTP\gamma S}$ (0.5 μM) from PC vesicles. Myristoylated ARF (0.5 μM) was incubated with 40 μM GTPγS and PC vesicles labeled with 5% DPH-PC (total phospholipid concentration: 160 μM) in buffer with 1 mM $MgCl_2$. ARF activation was triggered by the addition of 2 mM EDTA, and ARF binding to vesicles was followed by fluorescence energy transfer, as in Figure 4. When indicated, the concentration of free magnesium was raised back to 1 mM, by adding 2 mM $MgCl_2$, in order to stabilize the GTPγS-bound conformation. Then, a 5-fold excess of unlabeled vesicles was injected (white arrow) to follow the dissociation of $ARF_{GTP\gamma S}$ from the fluorescent labeled vesicles and its recruitment by the unlabeled vesicles. The decrease in fluorescence transfer can be fitted to a single exponential decay with $\tau_{off} = 90$ s. A second injection of unlabeled vesicles has no effect. In the upper part of the panel, the binding of [^{35}S]GTPγS to ARF (●) and the intrinsic tryptophan fluorescence of ARF (trace *b*) were measured under experimental conditions identical to that used in trace *a* except that unlabeled vesicles were used. These control experiments demonstrate that (i) the tryptophan fluorescence change observed at low [Mg] correlates exactly with the binding of [^{35}S]GTPγS under the same conditions; (ii) upon raising [Mg] to 1 mM, $ARF_{GTP\gamma S}$ is stabilized and does not release its bound GTPγS at a measurable rate ([^{35}S]GTPγS, tryptophan fluorescence, and fluorescence transfert traces are all stable); (iii) upon the addition of the 5-fold excess of unlabeled vesicles, GTPγS remains stable in ARF, ARF remains in the active conformation (trace *b* shows no change in ARF tryptophan fluorescence), but $ARF_{GTP\gamma S}$ dissociates from the labeled vesicles as it is recruited by the excessed unlabeled vesicle (decay of track *a*). (B) Effect of anionic phospholipids on the rate of $ARF_{GTP\gamma S}$ dissociation from vesicles. $ARF_{GTP\gamma S}$ dissociation from fluorescent labeled vesicles containing various amount of PG, PS, or PIP_2 was measured as in panel A. Error bars correspond to duplicate experiments with the same batch of lipid vesicles.

be involved in the interaction of $ARF_{GTP\gamma S}$ with membrane. Since the N-terminal peptide of ARF is essential for linking the conformational change of ARF to its binding to lipid vesicles (Kahn et al., 1992 and see above), it was tempting to assume that the hydrophobic residues of this amphipathic helix contribute to the binding of $ARF_{GTP\gamma S}$ to lipids. To test this hypothesis, we replaced some of these large hydrophobic residues by tryptophan, to further increase their hydrophobicity, or by alanines, to reduce it. Three mutants $^{[F9W]}$ARF, $^{[F9A]}$ARF, and $^{[L8A,F9A]}$ARF were constructed, and the myristoylated form was purified. These mutants exhibit properties that are qualitatively similar to that of wild-type myristoylated ARF: (i) they undergo GDP to GTP exchange only in the presence of lipids; (ii) they become membrane bound upon GTPγS binding. However, several quantitative differences are observed. When $^{[F9W]}$ARF binds to DPH-PC vesicles upon GDP/GTPγS exchange, fluorescence energy transfer to the lipid probe increases by 2-fold, as compared to wild-type ARF (Figure 6A). This is not due to a difference between the amounts of wild-type ARF and $^{[F9W]}$ARF that bind GTPγS and become membrane bound. The relative protein concentrations used in Figure 6A were adjusted according to a [^{35}S]GTPγS binding assay carried out under the same experimental conditions. Therefore, replacing Phe^9 by a tryptophan leads to a 2-fold increase in fluorescence transfer to the lipid probe. A similar effect was observed with all fluorescent probes tested (dansyl-PE and dipyrene-PC derivatives). The amplitude of the fluorescence transfer signal for the binding of $^{[F9A]}$ARF was significantly lower, whereas that of the double mutant $^{[L8A,F9A]}$ARF was nearly equal to that observed for wild-type ARF. However, for the $^{[F9A]}$ARF mutants, and in contrast to what is observed for $^{[F9W]}$ARF, this amplitude change is not due to a difference in the efficiency of transfer to the phospholipid probe but correlates with a reduced extent of GDP/GTPγS exchange, as monitored by a [^{35}S]GTPγS binding assay (data not shown). Significant effects of the mutations on the rate of GDP to GTPγS exchange kinetics were also observed. Exchange kinetics are 1.5 times faster for $^{[F9W]}$ARF, 13 times slower for $^{[F9A]}$ARF, and 3 times slower for the double mutant $^{[L8A,F9A]}$ARF than observed with wild-type ARF. These variations probably reflect conformational changes induced by the mutations in the N-terminal domain of ARF_{GDP}, which may affect unpredictably the rate of GDP release.

The effect of the mutations on the dissociation of $ARF_{GTP\gamma S}$ from the vesicles is much more significant: As shown above, wild-type $ARF_{GTP\gamma S}$ dissociates from vesicles containing 30% anionic phospholipids with a characteristic time constant of $\approx 225 \pm 25$ s. Under the same conditions, $^{[F9W]}ARF_{GTP\gamma S}$ dissociation was slowed down by a factor of 1.6. By contrast, the F9A mutant dissociates 7 times faster ($\tau_{off} = 30 \pm 5$ s) and the double mutant, L8A-F9A, does so 100 times faster ($\tau_{off} = 2.5 \pm 0.2$ s) (Figure 6B). Similar relative changes are observed when neutral (PC) vesicles are used instead of PC:PG vesicles. Thus, when the N-terminal helix is modified by point mutations, the interaction of $ARF_{GTP\gamma S}$ with the membrane changes according to the hydrophobicity of the mutated residues (Figure 6C).

DISCUSSION

The first aim of this study was to quantify the interaction between myristoylated ARF, either in the GDP state or in the GTP state, with unilamellar phospholipid vesicles of well-defined composition. We showed that ARF displays no marked specificity for any lipid, including PIP_2, and interacts with membrane through a combination of hydrophobic and nonspecific electrostatic interactions. Moreover, we showed that the dramatic enhancement in its affinity for membrane, which is correlated with the GTP-induced conformational change, is due to membrane exposure of its N-terminal hydrophobic residues. These results can be analyzed in light of recent reports on the interaction of lipid-modified proteins or model peptides with membrane.

The inactive, GDP-bound form of ARF binds weakly to lipid vesicles. This interaction requires the myristoylation

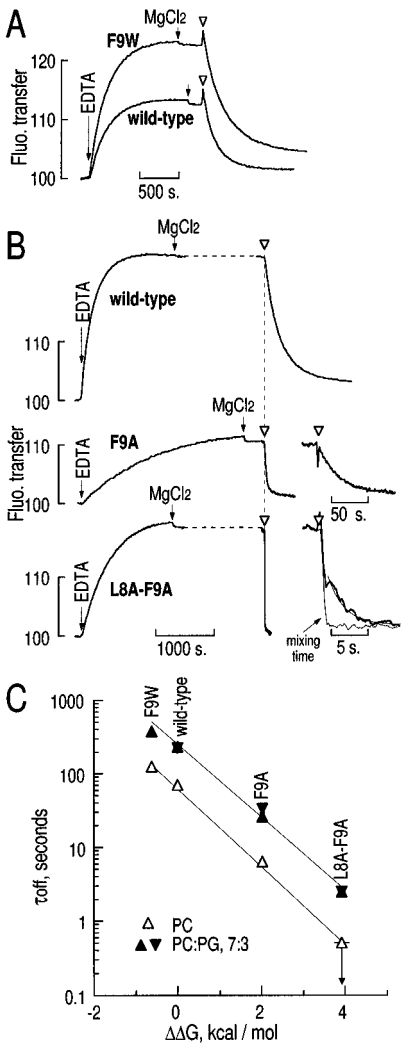

FIGURE 6: Effets of point mutations in the N-terminal helix of ARF on its binding to and dissociation from vesicles. Three mutants, $^{[F9W]}$ARF, $^{[F9A]}$ARF, and $^{[L8A-F9A]}$ARF, were compared to wild-type ARF for their binding to vesicles upon GDP to GTPγS exchange, and, in GTPγS-bound form, for their kinetics of dissociation from vesicles. The proteins were incubated with PC:PG:DPH-PC 65:30:5 vesicles in the presence of GTPγS. At the indicated time, EDTA (2 mM) was added and the binding of ARF to vesicles upon GDP to GTPγS exchange was followed by fluorescence energy transfer. Upon completion of the exchange, 2 mM $MgCl_2$ was added ($[Mg^{2+}]_{free} = 1$ mM) and a 5-fold excess of unlabeled vesicles was injected (white arrow head) to follow $ARF_{GTP\gamma S}$ dissociation from fluorescent-labeled vesicles. The kinetics of $^{[F9A]}ARF_{GTP\gamma S}$ and $^{[L8A-F9A]}ARF_{GTP\gamma S}$ dissociation from fluorescent-labeled vesicles are shown on an expanded time scale. The time course of $^{[L8A-F9A]}ARF_{GTP\gamma S}$ dissociation is very fast but is slower than the mixing time in the fluorescence cuvette which is about 0.5 s and which was measured here by the absorption signal of GTP when added to fluorescent labeled vesicles (thin trace). The protein concentration was 0.5 μM (A) or 1 μM (B), and the lipid concentration was 125 μM (A) or 250 μM (B). Vesicle batches used in panels A and B are different. (C) Rate of $ARF_{GTP\gamma S}$ dissociation from vesicles as a function of N-terminus hydrophobicity. Characteristic times, τ_{off}, of $ARF_{GTP\gamma S}$ dissociation from PC:PG:DPH-PC 65:30:5 vesicles (▲ and ▼, corresponding to different batches of lipid vesicles) or PC:DPH-PC 95:5 vesicles (△) are plotted as a function of the change in hydrophobicity ($\Delta\Delta G$) induced by each mutation. This change is calculated according to the data of Fauchere and Pliska (1983). τ_{off} value of $^{[L8A-F9A]}ARF_{GTP\gamma S}$ dissociation from PC vesicles is an upper limit due to instrumental limitation.

of ARF and the presence of anionic phospholipids (Figure 2). Thus, as in the case of other myristoylated proteins, such as Src or MARCKS (Sigal et al., 1994; Kim et al., 1994; Vergeres et al., 1995), the combination of the insertion of the myristate into the lipid bilayer and of nonspecific electrostatic interactions between cationic residues and negatively charged phospholipid heads leads to membrane binding. However, whereas Src and MARCKS display high affinity for charged vesicles (partition coefficients in the micromolar range), the affinity ARF_{GDP} for such vesicles is 1000 times lower (Figure 2). This difference could be explained by the accessibility of the myristoyl group and the number of basic residues that are involved in the interaction. Src displays a partition coefficient onto neutral membrane (100% PC) in the millimolar range due to the insertion of the myristate into the bilayer. By contrast, ARF_{GDP} does not bind significantly to neutral vesicles even at high PC concentration (10 mM PC), suggesting that the myristoyl group of ARF_{GDP} is less available for membrane insertion. A weak adsorption of myristate on the protein surface could be responsible for this effect. In the structure of ARF_{GDP}, five basic residues, including two lysines close to the N-terminal helix, form a patch of solvent-exposed positive charges that could interact with anionic phospholipids (Amor et al., 1994). In the case of Src and MARCKS, at least six and thirteen basic residues are known, respectively, to be involved in the interaction with membrane.

Two lines of evidence suggest that the dramatic enhancement in the affinity of ARF for membrane that occurs upon GDP to GTP exchange is mainly provided by hydrophobic residues. First, relatively low PC concentrations ($\approx$30 μM) are sufficient for ARF to switch from the GDP to the GTP state (Figure 3). At such concentrations, the insertion of the myristate is barely sufficient to anchor a simple myristoylated peptide into the membrane and, due to entropic cost, is insufficient to anchor myristoylated proteins such as MARCKS or Src (Peitzch & McLaughlin, 1993; Buser et al., 1994). Therefore, in addition to the insertion of the myristate into the bilayer, other additional hydrophobic interactions must be involved. But this argument is indirect: the activation of ARF is a complex mechanism which physiologically requires an exchange factor and which was studied here under artificial conditions (at micromolar magnesium). The direct argument in favor of an interaction between some ARF hydrophobic residues and the bilayer is given by the kinetics of $ARF_{GTP\gamma S}$ dissociation from neutral lipids vesicles. $ARF_{GTP\gamma S}$ dissociates from pure PC vesicles with a characteristic time of 75 $\pm$ 15 s (Figure 5). This τ_{off}, which depends only on the strength of hydrophobic interactions since no anionic lipids are present, cannot be explained by the sole insertion of myristate into the bilayer. The rates at which model peptides, carrying either one or two lipid modifications, dissociate from unilamellar vesicles have been extensively documented (Silvius & L'Heureux, 1994; Shahinian & Silvius, 1995). All known lipid modifications were examined, either alone or in combination. On the one hand, peptides carrying a single lipid modification bind to, as well as dissociate from, vesicles in the subsecond range. On the other hand, peptides carrying two lipid modifications show desorption times from hours to a few days. ARF carries only one lipid modification and, as compared with the other lipid modifications (farnesylation, geranylgeranylation, and palmitoylation), myristoylation is the least hydrophobic motif (Shahinian & Silvius, 1995). Therefore, the fact that $ARF_{GTP\gamma S}$ dissociates from PC membranes in about 1 min

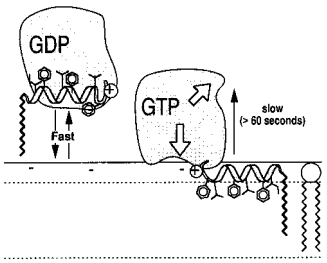

FIGURE 7: Model of the GTP-dependent binding of ARF to membranes. In the GDP state, ARF is mostly soluble but interacts transiently with membrane. Myristate inserts into the bilayer and a some basic residues (+) interacts electrostatically with acidic phospholipids such PS or PG (−). This weak interaction favors the interaction of ARF_{GDP} with the exchange factor. In the GTP-bound state, ARF is tightly bound to membranes. This long-lived interaction is due to exposure of ARF N-terminal hydrophobic residues. These residues, which are buried in the GDP-bound state and on the same face of an amphipatic helix (Amor et al. 1994), become available for anchor to the lipid bilayer when the protein switches to the GTP state. They provide the additional binding energy that, in addition to nonspecific electrostatic interactions and insertion of the myristoyl group, permits a stable association of ARF with the membrane. The large white arrows indicate that several regions must be affected by the conformational change: the classical "switch" domains, which control the binding to effectors, and the N-terminal helix, which controls the binding to membrane.

implies that hydrophobic residues are involved, in addition to myristate, in the binding to membranes.

We show here that two hydrophobic residues of the N-terminal helix, Leu^8 and Phe^9, which are buried in the protein in the ARF_{GDP} form, participate directly with the membrane binding by the active $ARF_{GTP\gamma S}$ form. Replacement of one or two of these hydrophobic residues with alanines accelerates the dissociation of $ARF_{GTP\gamma S}$ from vesicles by 1 or 2 orders of magnitude, whereas substitution of Phe^9 by Trp slows down $ARF_{GTP\gamma S}$ dissociation by a factor of 1.6 ± 0.1. A linear correlation is observed between these off rates and the calculated changes in hydrophobic binding energy with both neutral and charged lipid vesicles (Figure 6C). Thus, the "strength" of the interaction between $ARF_{GTP\gamma S}$ and membrane is directly correlated with the hydrophobicity of these residues in the N-terminal helix. In addition, the weak contribution of nonspecific electrostatic interactions in the binding of $ARF_{GTP\gamma S}$ to lipid membrane is not affected by the mutations: as in the case of wild-type ARF, introducing 30% PG in PC vesicles slows down the dissociation of each mutant by a factor of 3−4.

The structure of ARF_{GDP} shows that Leu^8 and Phe^9 as well as most of the hydrophobic residues of the N-terminal helix are buried in a hydrophobic pocket (Figure 1). The fact that they contribute to the binding of $ARF_{GTP\gamma S}$ to membranes suggests that the GTP-induced conformational change promotes the release of the N-terminal helix from its pocket and hence permits the insertion of three clusters of hydrophobic residues (I^4F^5, L^8F^9, and $L^{12}F^{13}$) into the lipid bilayer (Figure 7). We speculate that the helix lies parallel to the bilayer and that its hydrophobic residues insert at the level of phospholipid acyl chains. It has been shown that the peptide corresponding to the 13 N-terminal residues of ARF adopts a helical conformation when mixed with PC−cholate micelles (Kahn et al., 1992). Moreover, introduction of a single tryptophan in lieu of Phe^9 leads to a 2 times larger fluorescence transfer to various lipid probes (Figure 6A). Since wild-type ARF has four tryptophans, this suggests that the added tryptophan might be in the vinicity of the membrane. In addition to the insertion of hydrophobic residues, the two lysines that follow the N-terminal helix (K^{15} and K^{16}) may also contribute to membrane binding when anionic lipids are present and could be responsible for the moderate effect of electrostatic interactions on the rate of $ARF_{GTP\gamma S}$ dissociation from lipid vesicles.

The fact that ARF_{GTP} displays a very slow desorption rate from vesicles is interesting in view of the role of ARF in vesicular traffic. With artificial charged vesicles (PC:PG or PC:PS 70:30), myristoylated ARF_{GTP} is trapped on the same vesicle for 3−4 min. Vesicular transport in the Golgi occurs at time scale of about 1 min (Rothman & Wieland, 1996). Therefore, our results suggest that ARF_{GTP} remains associated with the same vesicle throughout the transport between two compartments, whereas ARF_{GDP} is rapidly released.

Whereas hydrophobic and, to a lesser extent, nonspecific electrostatic interactions of ARF lysines with charged lipid polar heads are involved in the interaction of ARF with membranes, we have no evidence for a specific interaction of ARF with PIP_2. We show that PIP_2 has no effect, other than strictly electrostatic, in (i) the weak binding of ARF_{GDP} to membranes, (ii) the spontaneous activation of ARF (Figure 3C), and (iii) the tight interaction of $ARF_{GTP\gamma S}$ with membrane (Figure 5B). These results are in marked contrast with that of Terui et al. (1994), who reported large effects of PIP_2 on the activation rate of ARF. Differences between experimental conditions could explain these contradictory results. We use PIP_2 as a minor component (up to 5%) homogeneously dispersed in unilamellar PC vesicles, whereas Terui et al. added large quantities of pure PIP_2 to PC−cholate micelles. In a recent study on the effect of PIP_2 on G-protein-coupled receptor kinases, Pitcher et al. (1996) have shown that such differences in the manner in which PIP_2 is presented can lead to opposite results. Since only few percent of PIP_2 are present in membranes, the use of pure PIP_2 or high mole fraction of this highly charged lipid is questionable. Indeed, our recent characterization of the PIP_2 sensitive ARF nucleotide exchange factor ARNO (Chardin et al., 1996) has allowed us to show that PIP_2 is involved indirectly, rather than directly, in the control of the GDP/GTP cycle of ARF. This exchange factor binds through a N-terminal PH domain to PIP_2-containing vesicles. Incorporating a few percent of PIP_2 in PC:PG vesicles dramatically increases the activity of ARNO on ARF. This increase in activity is probably not due to a PIP_2-induced conformational change but rather to a reduction in dimensionality, as in the case of PLCδ (Ferguson et al., 1995; Garcia et al., 1995). Membrane binding of ARNO, through PIP_2−PH domain interaction, and of ARF_{GDP}, through myristate insertion, would favor the interaction between these two proteins and hence facilitates ARF activation (Franco et al., 1996; Chardin et al., 1996).

The binding of myristoylated proteins to membranes can be controlled by several mechanisms. In the case of recoverin, exposure of myristate is directly controlled by a Ca^{2+}-dependent conformational change (Tanaka et al., 1995; Hugues et al., 1995). In the case of MARCKS, phosphorylation weakens electrostatic interactions of the basic domain with acidic phospholipids and induces MARCKS desorption from membranes (Kim et al., 1994). For hisactophilin, a cluster of histidine residues permits a pH-dependent binding to lipid membranes (Hanakam et al., 1996). ARF provides

a fourth type of mechanism, in which membrane binding is controlled by a GTP-dependent exposure of hydrophobic residues.

ACKNOWLEDGMENT

We thank Sonia Paris and M. Vuong for very helpful discussions and comments on the manuscript, Sonia Paris for GTPγS binding assays, Joëlle Bigay for preparing $^{[\Delta 17]}$ARF, and Isabelle Lenoir and Nordine Belmokhtar for excellent technical assistance.

REFERENCES

Amor, J. C., Harrison, D. H., Kahn, R. A., & Ringe, D. (1994) *Nature 372*, 704−708.

Antonny, B., Chardin, P., Roux, M., & Chabre, M. (1991) *Biochemistry 30*, 8287−8295.

Bourne, H. R., Sanders, D. A., & McCormick, F. (1991) *Nature 349*, 117−127.

Buser, C. A., Sigal, C. T., Resh, M. D., & McLauglin, S. (1994) *Biochemistry 33*, 13093−13101.

Chardin, P., Paris, S., Antonny, B., Robineau, S., Beraud-Dufour, S., Jackson, C. L., & Chabre, M. (1996) *Nature 384*, 481−484.

Fauchere, J.-L., & Pliska, V. (1983) *Eur. J. Med. Chem. 18*, 369−375.

Faurobert, E., Otto-Bruc, A., Chardin, P., & Chabre, M. (1993) *EMBO J. 12*, 4191−4198.

Ferguson, K. M., Lemmon, M. A., Schlessinger, J., & Sigler, P. B. (1995) *Cell 83*, 1037−1046.

Franco, M., Chardin, P., Chabre, M., & Paris, S. (1993) *J. Biol. Chem. 268*, 24531−24534.

Franco, M., Chardin, P., Chabre, M., & Paris, S. (1995) *J. Biol. Chem. 270*, 1337−1341.

Franco, M., Chardin, P., Chabre, M., & Paris, S. (1996) *J. Biol. Chem. 271*, 1573−1578.

Garcia, P., Gupta, R., Shah, S., Morris, A. J., Rudge, S. A., Scarlata, S., Petrova, V., McLaughlin, S., & Rebecchi, M. J. (1995) *Biochemistry 34*, 16228−16234.

Greasey, S. E., Jhoti, H., Teahan, C., Solari, R., Fensome, A., Thomas, G. M., Cockroft, S., & Bax, B. (1995) *Nat. Struct. Biol. 2*, 797−806.

Hanakam, F., Gerisch, G., Lotz, S., Alt, T., & Seelig, A. (1996) *Biochemistry 35*, 11036−11044.

Herrmann, C., Martin, G. A., & Wittinghofer, A. (1995) *J. Biol. Chem. 270*, 2901−2905.

Higashijima, T., Ferguson, K. M., Sternweis, P. C., Ross, E. M., Smigel, M. D., & Gilman, A. G. (1987) *J. Biol. Chem. 262*, 752−756.

Hope, M. J., Bally, M. B., Webb, G., & Cullis, P. R. (1985) *Biochim. Biophys. Acta 812*, 55−65.

Hughes, R. E., Brzovic, P. S., Klevit, R. E., & Hurley, J. B. (1995) *Biochemistry 34*, 11410−11416.

Kahn, R. A., & Gilman, A. G. (1986) *J. Biol. Chem. 261*, 7906−7911.

Kahn, R. A., Randazzo, P., Serafini, T., Weiss, O., Rulka, C., Clarck, J., Amherdt, M., Roller, P., Orci, L., & Rothman, J. E. (1992) *J. Biol. Chem. 267*, 13039−13046.

Kim, J., Shishido, T., Jiang, X., Aderem, A., & McLaughlin, S. (1994) *J. Biol. Chem. 269*, 28214−28219.

Kraulis, P. J. (1991) *J. Appl. Crystallogr. 24*, 946−950.

Ktistakis, N. T., Brown, H. A., Waters, M. G., Sternweis, P. C., & Roth, M. G. (1996) *J. Cell Biol. 134*, 295−306.

Lu, Y., & Nelsestuen, G. (1996) *Biochemistry 35*, 8193−8200.

MacDonald, R. C., MacDonald, R. I., Menco, B. P., Takeshita, K., Subbarao, N. K., & Hu, L.-R. (1991) *Biochim. Biophys. Acta 1061*, 297−303.

McLaughlin, S., & Aderem, A. (1995) *Trends Biochem. Sci. 20*, 272−276.

Moss, J., & Vaughan, M. (1995) *J. Biol. Chem. 270*, 12327−12330.

Otto-Bruc, A., Antonny, B., Chardin, P., Vuong, T. M., & Chabre, M. (1993) *Biochemistry* 32, 8636−8645.

Peitzch, R. M., & McLaughlin, S. (1993) *Biochemistry 32*, 10436−10443.

Pitcher, J. A., Fredericks, Z. L., Stone, W. C., Premont, R. T., Stoffel, R. H., Koch, W. J., & Lefkowitz, R. J. (1996) *J. Biol. Chem. 271*, 24907−24913.

Randazzo, P., Terui, T., Sturch, S., Fales, H. M., Ferrige, A. G., & Kahn, R. A. (1995) *J. Biol. Chem 270*, 14809−14815.

Rothman, J. E., & Wieland, F. T. (1996) *Science 272*, 227−233.

Shahinian, S., & Silvius, J. R. (1995) *Biochemistry 34*, 3813−3822.

Sigal, C. T., Zhou, W., Buser, C. A., McLaughlin, S., & Resh, M. D. (1994) *Proc. Natl. Acad. Sci. U.S.A. 91*, 12253−12257.

Silvius, J. R., & L'Heureux F. (1994) *Biochemistry 33*, 3014−3022.

Tanaka, T., Ames, J., Harvey, T. S., Stryer, L., & Ikura, M. (1995) *Nature 376*, 444−447.

Terui, T., Kahn, R. A., & Randazzo, P. A. (1994) *J. Biol. Chem. 269*, 28130−28135.

Vergeres, G., Manenti, S., Weber, T., & Stürzinger, C. (1995) *J. Biol. Chem. 270*, 19879−19887.

Walker, M. W., Bobak, D. A., Tsai, S.-C, Moss, J., & Vaughan, M. (1992) *J. Biol. Chem. 267*, 3230−3235.

BI962252B